

Orbital masses of nearby luminous galaxies

Igor D. Karachentsev

Special Astrophysical Observatory, Russian Academy of Sciences, Russia

Yuri N.Kudrya

Taras Shevchenko National University of Kyiv, Ukraine

ikar@sao.ru

ABSTRACT

We use observational properties of galaxies accumulated in the Updated Nearby Galaxy Catalog to derive a dark matter mass of luminous galaxies via motions of their companions. The data on orbital-to-stellar mass ratio are presented for 15 luminous galaxies situated within 11 Mpc from us: the Milky Way, M31, M81, NGC5128, IC342, NGC253, NGC4736, NGC5236, NGC6946, M101, NGC4258, NGC4594, NGC3115, NGC3627 and NGC3368, as well as for a composit suite around other nearby galaxies of moderate and low luminosity. The typical ratio for them is $M_{orb}/M_* = 31$, corresponding to the mean local density of matter $\Omega_m = 0.09$, i.e 1/3 of the global cosmic density. This quantity seems to be rather an upper limit of dark matter density, since the peripheric population of the suites may suffer from the presence of fictitious unbound members. We notice that the Milky Way and M31 haloes have lower dimensions and lower stellar masses than those of other 13 nearby luminous galaxies. However, the dark-to-stellar mass ratio for both the Milky Way and M31 is the typical one for other neighboring luminous galaxies. The distortion in the Hubble flow, observed around the Local Group and five other neighboring groups yields their total masses within the radius of zero velocity surface, R_0 , which are slightly lower than the orbital and virial values. This difference may be due to the effect of dark energy, producing a kind of “mass defect” within R_0 .

Key words: cosmology: observations - dark matter - galaxies: groups: general

Subject headings: cosmology: observations - dark matter - galaxies: groups: general

1. Introduction

In spite of tremendous success of observational cosmology, reached over the past quarter century, many issues regarding the nature of dark matter and its distribution in the universe relative to the visible (stellar) matter still remain unresolved. Numerous studies (Karachentsev 1966, Rood

et al. 1970, Bahcall et al. 2000) have shown that in groups and clusters of galaxies the ratio of dark (virial) mass to stellar mass systematically increases with size and population of a given system of galaxies. In the richest clusters, such as the Coma, the M_{DM}/M_* ratio reaches up to two orders of magnitude. If all the galaxies are part of clusters, dark matter associated with them would provide the average density of matter in space amounting to $\Omega_m \simeq 0.26$ (Bahcall & Kulier, 2014), corresponding to the standard cosmological Λ CDM model (Spergel et al. 2007).

However, no more than 10% of all galaxies belong to rich clusters (Libeskind et al, 2013, Cautun et al. 2014). Most of them are included in groups of different multiplicity, which are concentrated in the filaments and “sheets”, forming a large-scale “cosmic web” (Bond et al. 1996, Shandarin et al. 2004, Einasto et al. 2011). Looking at the data on 11000 galaxies of the nearby universe with radial velocities $V_{LG} \leq 3500 \text{ kms}^{-1}$, Makarov & Karachentsev (2011) have identified in this volume about 400 groups and clusters of galaxies and determined their virial masses. The summation of virial masses of groups and clusters in the volume of ~ 50 Mpc radius led to the average density estimate of $\Omega_m(\text{local}) \simeq 0.08 \pm 0.02$, which is three times lower than the global cosmic density. This result confirmed the earlier estimates of $\Omega_m \sim (0.08 - 0.10)$, which were obtained for the Local universe by Vennik (1984), Tully (1987), Magtesian (1988) and other authors. A threefold difference between the estimates of $\Omega_m(\text{local})$ and $\Omega_m(\text{global})$ did not cause much concern among theorists. It was considered quite obvious that dark matter is not distributed in clusters and groups with the same concentration as stellar matter (biasing effect). Darker peripheries of the clusters probably contain a large amount of dark matter, the presence of which eliminates the paradox of “missing dark matter”.

The assumption of massive dark halos existing around the clusters and groups of galaxies is not, however, confirmed by the observations. Investigating the Hubble flow of galaxies around the Virgo, the nearest cluster of galaxies, Karachentsev et al. (2014b) showed that the total mass of the cluster, determined from the external motions of galaxies is in a good agreement with the virial mass estimate based on the motions within the cluster. Since the total mass of the Virgo cluster was estimated on a scale of the “zero velocity sphere” radius, R_0 , which is ~ 3.7 times larger than the virial radius R_v , this result gives evidence against the localization of a significant amount of dark matter in the layer between R_v and R_0 . A similar situation occurs around the Local Group of galaxies (Karachentsev et al. 2009). Consequently, we should be on the outlook for other ideas and observational data to resolve the paradox of missing dark matter.

The recently published “Updated Nearby Galaxy Catalog” = UNGC, (Karachentsev et al., 2013) contains a summary of data on radial velocities, distances and other observable parameters of about 800 galaxies located within a 11 Mpc radius around us. More than 300 galaxies of this sample have accurate distance measurements with a better than 10% accuracy obtained by the Tip of the Red Giant Branch from observations with the Hubble Space Telescope. Due to the proximity of the UNGC- objects, the kinematic data density in the catalog proves to be 6 times higher than in the sample of the nearby ($D \leq 50$ Mpc) universe (Makarov & Karachentsev, 2011, hereafter MK11). This circumstance, and the presence of individual distance measurements in

many UNGC galaxies allows us to investigate the structure of nearby groups and their vicinities with unprecedented detail. Determining the masses of the most nearby galaxies from the motions of their companions is the main subject of this paper.

2. Projected and orbital mass estimates

To determine the mass of a system of N point-like bodies, one usually uses the virial theorem in the form of

$$M_v = (3\pi/2) \times G^{-1} \times S_v^2 \times R_h^{-1}, \quad (1)$$

where G is the gravitational constant, S_v^2 is the velocity dispersion on the line of sight, R_h is the average harmonic separation between the group members in the projection on the sky, and $(3\pi/2)$ is the average projection factor at arbitrary group orientation with respect to the line of sight (Bahcall & Tremaine, 1981). But this estimator is statistically offset and inefficient. Therefore, Heisler et al. (1985) proposed to estimate the mass of a group in a more robust way:

$$M_p = (32/\pi) \times N \times (N - 3/2)^{-1} G^{-1} \langle \Delta V^2 \times R_p \rangle, \quad (2)$$

where M_p is the so-called “projected” mass, N is the number of objects, and $\langle \Delta V^2 \times R_p \rangle$ is the average product of squared radial velocity of the component relative to the group center, and its projection separation from the center. Both these mass estimators presume spherical symmetry of the groups as well as isotropic velocity distribution. But as shown by Wojtak (2013) many groups are highly aspherical, with shapes approximately by nearly prolate ellipsoids. According to Wojtak (2013) their mean spatial axial ratio is ~ 0.66 and the mean axial ratio of the velocity ellipsoids is ~ 0.78 . Furthermore, simulated dark matter haloes tend to be aligned with the cosmic web in the way that the semi-major axis is aligned with the local filaments and the semi-minor axis is pointing to neighbouring voids (Libeskind et al. 2013). Being mostly located in the Local Sheet, the nearby groups may be preferentially observed along their major or median axis that would have any effect on the mass estimates.

If the group is dominated by a massive galaxy, surrounded by a set of test particles with random orientation of their orbits, one can use the “orbital” mass estimate (Karachentsev, 2005):

$$M_{orb} = (32/3\pi)(1 - 2e^2/3)^{-1} \times G^{-1} \times \langle \Delta V_{12}^2 \times R_{p12} \rangle, \quad (3)$$

where ΔV_{12} and R_{p12} are the velocity difference and the projected separation of companions relative to the main galaxy, and e is the prevailing orbit eccentricity. Assuming the typical eccentricity value of $\langle e^2 \rangle \simeq 1/2$ (Barber et al. 2014), we get

$$M_{orb} = (16/\pi) \times G^{-1} \times \langle \Delta V_{12}^2 \times R_{p12} \rangle. \quad (4)$$

For completeness, we also mention another approach to mass estimation proposed by Be-
 laborodov & Levin (2004). Based on the natural assumption that companions of the main galaxy
 are observed at random orbital phase moments, they offered so-called “orbital roulette estimator”

$$M_{rlt} = 6 \times (2 - \langle e^2 \rangle)^{-1} \times G^{-1} \times \langle \Delta V_{12}^2 \times R_{p12} \rangle, \quad (5)$$

which uses just the same observables, but yields at $\langle e^2 \rangle = 1/2$ the mass estimate 21% smaller
 than (4). Note that at $N = 2$ the projected mass estimate (2) coincides with the orbital estimate
 (4). We will use the orbital mass estimator further on.

3. Neighboring giants and their suites

Possessing the data on the distances and luminosities of 869 galaxies of the Local Volume,
 Karachentsev et al. (2013) have determined for each galaxy its tidal index

$$\Theta_1 = \max[\log(M_n^*/D_n^3)] + C, \quad n = 1, 2, \dots, N, \quad (6)$$

where M^* is the stellar mass of the neighboring galaxy, and D_n is its spatial separation from the
 considered galaxy. The stellar mass of the galaxy was assumed to be equal to its K-band luminosity
 at $M^*/L_K = 1M_\odot/L_\odot$ (Bell et al, 2003). Ranking the surrounding galaxies by the magnitude of
 their tidal force, $F_n \sim M^*/D_n^3$, allowed to find the most influential neighbor, called the Main
 Disturber (= MD). Here the ratio of the total mass of the galaxy to its stellar mass was considered
 to be constant regardless of the luminosity and morphology of galaxies. The constant $C = -10.96$ in
 equation (6) was chosen so that the galaxy with $\Theta_1 = 0$ was located at the “zero velocity sphere”
 relative to its MD. In other words, the galaxy with $\Theta_1 > 0$ was regarded as causally (gravitationally)
 related to its MD as their crossing time was shorter than the age of the universe, $T_0 = 13.7$ Gyr.
 Consequently, the causally unrelated galaxies with $\Theta_1 < 0$ were referred to as the population of
 “general field”.

Obviously, the galaxies which have a common MD can be combined in a certain association, or
 a MD “suite”. At that, an aggregate of suite members with positive Θ_1 values is quite consistent
 with the notion of a physically bound group of galaxies. Karachentsev et al. (2014a) have analyzed
 different properties of galaxies in the suites, as well as properties of their main galaxies. As expected,
 the most massive MDs possess the most populous suites. The total number of companions around
 15 most massive galaxies makes up about a half of the total population of the Local Volume.

The full list of suites, ranked by the number of suite members from $n = 53$ to $n = 1$ is presented
 in Table 1 (Karachentsev et al. 2014a). ¹ The Table 5 (Appendix) below presents the summary of

¹Its machine-readable version is available at http://lv.sao.ru/lvgdb/article/suites_dw_Table1.txt.

15 richest groups (suites) of the Local Volume, in which at least 6 galaxies have measured radial velocities. We did not include in the Table 5 those members of suites, which radial velocities remain still unmeasured. These cases consist of about 1/3 of the total amount of suite members.

The heading line of each suite presents: the name of the Main Disturber, its distance in Mpc, its stellar mass and the value of orbital mass with the standard error. The suites (groups) are arranged in the descending order of their total population. The following is given for the members of each suite: (1) name of the galaxy in UNGC catalog; (2) the tidal index Θ_1 by which the members of the suite are ranked; (3) projection separation of the suite member from the MD in kpc, assuming that all the companions of the MD are at the same distance from the observer as the MD itself; (4) absolute value of the radial velocity difference of member of the suite and the MD in km/s.

The distribution of 351 companions by the radial velocity difference and projection separation relative to their main galaxies is presented in three panels of Fig.1. The upper panel of the figure shows the $\{|\Delta V|, R_p\}$ diagram for 31 companions of the Milky Way = MW (squares) and 39 members of the M 31 = Andromeda suite (diamonds). The companions of massive galaxies with the tidal index $\Theta \geq 0$, considered to be physical, are represented by closed symbols, while the members of the suites with $-0.5 < \Theta_1 < 0$ are shown by the open symbols. The extension of the companion sample by the objects with slightly negative values of Θ_1 was done not to miss some possible physical members of the group, in which the distances are as yet measured with low accuracy. The objects in this boundary category may appear to be both the real companions of main galaxies or belong to the population of general field. Note that for the MW companions we are not listing the spatial distances, but their projection on the plane perpendicular to the line of sight towards the MW center.

The middle panel of Fig.1 shows the $\{|\Delta V|, R_p\}$ distribution for 174 members of rich suites around 13 other massive nearby galaxies. Prospective physical companions with $\Theta_1 \geq 0$ (N=142) are also marked here by solid symbols.

In addition to 15 rich suites, the Local Volume comprises a lot of small suites, where the radial velocities are measured in one or several presumed companions. We have combined these small suites in a composite (“synthetic”) suite. The $\{|\Delta V|, R_p\}$ diagram for 107 companions uniting small suites is represented on the lower panel of Fig. 1. At that, we only kept the cases where the stellar mass of companion does not exceed half the mass of the main galaxy.

The dashed lines in all the three panels of Fig.1 show quadratic regressions of the velocity difference on the projection separation of companions. For the suites of galaxies around MW and M31, the regression has a negative slope. While for the synthetic suite of 142 companions around the 13 most massive galaxies and for the synthetic suite, uniting small suites, regressions show a weak increase in velocity dispersion from the center to the suite periphery. Different behavior of the regressions may indicate the atypical character of motion of the MW and M31 companions in comparison to the suites of other massive nearby galaxies. Another reason of the rising part of the

velocity dispersion may be caused by the presence of large scale halo when nearby groups are a part of larger structure, the Local Sheet, which would give rise to the observed enhancement of the velocity dispersion at large radii. However, a more obvious reason for this phenomenon is caused by the presence on the suite outskirts of an admixture of some false members entering the suites from the general field.

The basic characteristics of the considered suites are presented in Table 1. Its columns contain: (1) name of the suite/group by its main galaxy, (2) the number of physical ($\Theta_1 \geq 0$) members of the group with measured radial velocities, (3) the average projection separation of the companions from the main galaxy (kpc), (4) the mean absolute value of the radial velocity difference of the companions relative to the main galaxy (km/s), (5) the main galaxy stellar mass in the units of $10^{10}M_\odot$, (6) the value of orbital mass of the group (suite) in the units of $10^{12}M_\odot$ and its standard error coming from the error of the mean in equation (4). The location of suites in Table 1 corresponds to their breakdown in the three panels of Fig. 1: the first lines contain the data for the MW and M31 groups, followed by the characteristics of 13 other most populated groups of the Local Volume, and the end of the table shows the average parameters of composite suite. Since the main galaxies in the composite suite significantly differ by their stellar mass, we have divided the synthetic suite into three subsamples having about the same number of companions with measured radial velocities.

Distribution of the surface number density of 297 companions along the radius of the combined suite is presented in Fig. 2 in the log-log scale. The solid circles correspond to the number of physical companions, and the crosses consider the additional number of suite members with $\Theta_1 = [0, -0.5]$. The vertical bars show the statistical error of $\sqrt{N-1}$. The dashed line represents the quadratic regression

$$\log \Sigma(R_p) = -3.88 - 2.18 x - 0.56 x^2,$$

where $x = \log(R_p/200 \text{ kpc})$.

As can be seen, the surface number density profile for the synthetic suite is well compatible with the radial profile of the surface mass density for the standard NFW-profile of the dark halo (Navarro et al. 1997, Wang et al. 2014), as given by equation (41) and Figure 8 in Lokas & Mamon (2001).

4. Milky Way and Andromeda suites as compared with others

Modeling the structure and kinematics of galaxy groups within the Λ CDM paradigm, many authors (Libeskind et al. 2010, Zavala et al. 2009, Knebe et al. 2011) choose the Local Group to make a comparison with the observational data. As known, the Local Group has two gravitating centers: the MW and M31, which are approaching each other with mutual velocity of about 110

km/s. This binary character is not an exclusive feature. For example, the neighboring groups: M81 and NGC 2403, IC 342 and Maffei I, NGC 5128 and NGC 5236 also belong to the class of binary merging groups. But from the standpoint of the group mass estimate from the orbital motions of the companions, the listed galaxies have to be considered as standalone dynamical centers.

Previously Karachentsev et al. (2014a) noted that judging on some morphological features the groups of galaxies around the MW and M31 are not quite typical. This primarily refers to the presence near the MW of two companions (Magellanic Clouds) rich in gas. There are also other features that distinguish the MW and M31 groups among other nearby ones.

Six histograms of Fig.3 represent the distributions of 15 most populated suites in the Local Volume based on the following parameters: the average projected separation of the companions from the main galaxy, $\langle R_p \rangle$, the mean absolute value of the radial velocity difference of the companion and the main galaxy, the logarithm of stellar mass of the MD, the MD orbital mass, the ratio of the orbital mass-to-sum of stellar masses of all the galaxies in the group, $M_{orb}/\Sigma M_*$, and the average crossing time $t_{cr} = R_p/\sigma_v$ for the suite members, where t_{cr} is expressed in terms of the age of the universe, $T_0 = 13.7$ Gyr. The groups of galaxies around the MW and Andromeda are marked with “M” and “A”, respectively.

According to these data, the linear dimension of the suites around MW and M31 are approximately 2 times less extended than the typical suite of other neighboring massive galaxies. In the case of MW, that can be caused by the obvious selection effect: most of the recently discovered ultra-low luminosity companions of the MW were found at the distances of less than 100 kpc (Willman et al. 2005, Belokurov et al. 2006). To some extent, the small linear size of the suite of companions around M31 can also be caused by a selection effect, since the most thorough search for new companions was carried out in a limited region around M31 (Ibata et al. 2007, Martin et al. 2009). However, the most plausible explanation of this difference may also be the presence in the suites of neighboring massive galaxies of a certain number of false members, which appear on the periphery of the suites from the general field.

In contrast to the linear dimensions, radial velocity dispersion for the companions of MW and M31 does not stand out among the other groups (panel “b”).

The “c” histogram data show that based on their stellar masses, both MW and M31 do not get in the top ten most massive galaxies of the Local Volume. This may be also the reason of understated linear dimensions of the suites around the MW and M31.

The “d” and “e” histograms show the distribution of 15 suites by the orbital mass and by the ratio of the orbital mass-to-sum of stellar masses of the group members, respectively. The two groups located most rightward on these panels correspond to the suite around NGC 4594 (“Sombrero”) and the group NGC 3368/3379 (Leo I).

If in the distribution of suites by the value of M_{orb} both groups MW and M31 are shifted towards the lower values relative to the average, whereas based on the $M_{orb}/\Sigma M_*$ parameter, both

groups are not significantly different from the rest.

The lower panel of Fig.3 shows the distribution of suites by the average crossing time of the companions. A typical dynamic situation in the group of the Local Volume is expressed by the fact that the companions of massive galaxies have time to make about 5 oscillations around the center, which is sufficient for the group to get virialized. Two suites on the right side of the histogram with $t_{cr} \sim 1/2$ are the scattered groups around NGC 253 (the Sculptor filament) and NGC 4736 (the CVn I cloud), the dynamical relaxation of which has apparently not yet achieved.

5. Orbital and projected masses of neighboring groups

As noted above, the formation of suites around the nearby galaxies was made based on the data on mutual separations and stellar masses (L_K -luminosities) of galaxies in the Local Volume. Radial velocities of galaxies were not taken into account here. Among ~ 400 groups from the list of MK11 there are fairly nearby groups falling into the Local Volume. In 18 of them the number of members with known radial velocities is not too small ($N_v \geq 4$) to estimate the projected mass of the group with an acceptable statistical error. The sample of these 18 groups presents a unique opportunity to compare the dynamical mass estimates made applying different methods to the systems of galaxies, the principles of identification of which were essentially different.

Let us recall that the arrangement of galaxies in MK-groups was carried out via the pairwise revision of all galaxies with two conditions: the total energy of a virtual bound pair must be negative, and the pair components have to be within the “zero velocity sphere,” determined by the total mass of the pair. In the space of projected separations R_p and radial velocity differences ΔV_{12} , these conditions are expressed as

$$\Delta V_{12}^2 R_p < 2G(M_1 + M_2), \quad (7)$$

$$\pi H_0^2 R_p < 8G(M_1 + M_2), \quad (8)$$

where the condition

$$M/M_* = \kappa = 6 \quad (9)$$

was assumed for the relation of the dynamical mass of each galaxy to its stellar mass.

Then, all the virtual bound pairs with common members were united in a group. Unlike another widely used method of organizing the galaxies in “friends of friends” groups (Huchra & Geller 1982, Crook et al. 2007), the (7) – (9) criterion contains only one arbitrary dimensionless parameter κ . At the empirically selected value of $\kappa = 6$, the (7)–(9) criterion brings together in pairs, groups and clusters about 54% of all galaxies, what is in good agreement with the observed structure of the Local Volume (see the details in the MK11).

A comparison of parameters of the suites around 18 nearby massive galaxies with the characteristics of the corresponding nearby MK-groups is given in Table 2. The top rows of the table represent the data for the MK-groups, while the lower rows list the parameters of the suites. The columns contain: (1) name of the main galaxy of the group/suite; (2) number of galaxies in the group/suite with measured radial velocities; (3) the distance to the group (Mpc), determined by the mean radial velocity of the group members relative to the Local Group centroid at $H_0 = 73$ km/s/Mpc, and the individual distance of the principal galaxy of the suite; (4) dispersion of radial velocities in the group and the mean-square difference of the companion velocities relative to the main galaxy (km/s); (5) the mean harmonic radius of the group and the mean projection separation of companions from the main galaxy (kpc); (6) logarithm of the total stellar mass of the group or the suite (in M_\odot); (7) logarithm of the projected mass of the group and the orbital mass of the suite (in M_\odot); (8) the ratio of the projected (or orbital) mass-to-total stellar mass in the logarithmic scale; (9) morphological type of the main galaxy on de Vaucouleurs scale; (10) difference between apparent K-magnitudes of the first and second members of the group; (11–13) the tidal indices, characterizing the environment density of the main galaxy in the group: here the Θ_1 index, determined by equation (6), expresses the contribution of the most significant neighbor, the Θ_5 index accounts for the effect of five important neighbors, while the Θ_J index corresponds to the logarithm of stellar density contrast in a sphere of 1 Mpc radius around the main galaxy taken with respect to the mean cosmic density. The last line in the table shows the mean values of the considered quantities. Note that the luminosity of the brightest suite member does not exceed 1/4 of the MD’s luminosity for 10 of the 15 suites, that justifies the consideration of suite galaxies as test particles orbiting around the central massive body.

One can notice that Table 2 has no data on the groups around IC 342 and NGC 6946. They are not included in the list of MK-groups because located in the zone of strong Galactic extinction. The groups of companions around the MW and M31 are also missed because their distances based on the mean radial velocities of the galaxies, used by Makarov & Karachentsev (2011), would have no physical meaning. A comparison of the Table 2 data on the groups versus the suites reveals the following properties.

a) The total number of galaxies in the MK-groups, 227, is comparable to the total number of physical members of the suites: 170 at $\Theta_1 > 0$ and 224 at $\Theta_1 > -0.5$. Consequently, the association of galaxies into suites by the zones of gravitational influence around dominant galaxies, and by the MK-criterion (7–9) have approximately the same clustering efficiency rate. However, the data presented reveal also significant individual differences in the populations of groups and suites. For example, in the NGC 891, NGC 4631 and NGC 4736 groups, this ratio amounts to 18:4, 28:5 and 5:15, respectively. The greatest differences are typical for the scattered groups (suites), where the second member of the group by luminosity competes with the MD.

b) The mean radial velocity dispersion in groups, equal to 83 km/s, and the mean square velocity difference of the companions in the suites, amounting to 99 km/s, are in a reasonable agreement with each other. In other words, condition (7) in the MK-criterion does not possess

strong selectivity against the pairs of galaxies with a large radial velocity difference.

c) The difference between the Hubble distance to the groups, $D_H = \langle V_{LG} \rangle / H_0$, and individually measured distance to the main galaxy of the suite, D_{MD} , is on the average small: 7.44 Mpc and 7.39 Mpc, respectively. While in some groups, for instance, in NGC 628 and NGC 2903, these distances differ by half (due to the bulk motions towards the Virgo cluster), which affects the luminosity of the group and influences the number of clustered members in it.

d) Individual differences between the estimates of the projected mass and orbital mass are quite large. In the case of groups of galaxies around NGC 253, NGC 891, NGC 3627, NGC 4594, NGC 4736 and NGC 5194, these differences exceed the factor 3. Nevertheless, the average values of $\langle \log M_p \rangle = 12.44$ and $\langle \log M_{orb} \rangle = 12.41$ for an ensemble of 18 groups/suites are in good agreement with each other. Similarly, the average ratios of $\langle \log(M_p / \Sigma M^*) \rangle = 1.50$ and $\langle \log(M_{orb} / \Sigma M^*) \rangle = 1.53$ do not show any significant systematic difference, although in some groups/suites these ratios differ significantly. In addition to random factors caused by the poor statistics, the differences in the estimates of M_{orb} and M_p occur more in scattered groups, where we can discern the substructures around the galaxies, which are only slightly less massive than the main member of the group. The examples revealing the presence of such hierarchical substructures can be found in the NGC 891/NGC 925, NGC 3368/NGC 3379 and NGC 5194/NGC 5055 groups.

e) The data of the last columns of Table 2 show that the density of the group environment, the difference in the apparent magnitudes of two brightest members of the group, and the morphological type of the main galaxy do not affect the ratio of dark-to-luminous matter in the group in a substantial way.

It should be emphasized that the derived above agreement between the typical values of orbital and projected masses in the Local Volume, $M_{orb} \simeq M_p \simeq 33M^*$, is not trivial one. The UNGC catalog contains approximately the same number of radial velocities as what was used by MK11 within $D < 11$ Mpc. However, the UNGC has much more data on galaxy distances than MK11 sample. Actually, MK11 estimated distances to a group via the average redshift of its members burdened by peculiar velocities and local streams. This is does not matter in the case of UNGC which collected hundreds accurate individual distances. Another significant difference is caused by different algorithms applied to the galaxy grouping. To find a group, MK11 used as separations and luminosities of galaxies, as well their radial velocities. In the case of UNGC, only 3D-separations and luminosities (but not redshifts) were used to identify a suite of companions around a dominant galaxy. We can not state that one finding algorithm is better (or objective) than the other. But they both yield almost the same average ratio M_{DM}/M^* for the small local structures.

6. Orbital-to-stellar mass ratios

The orbital mass estimates for the populated suites, shown in Tables 1 and 2, were determined by the suite members with tidal indices $\Theta_1 \geq 0$. Obviously, the choice of the maximum value of

Θ_1 , based on which the galaxies were included in the suite, affects the number of members of the suite, their total luminosity, and the orbital mass estimate. With large positive values of Θ_1 , many physical companions of the MD do not make it in its suite. The orbital mass would in this case prove to be underestimated. On the contrary, inclusion of galaxies with arbitrary negative values of Θ_1 in the suite contributes to its pollution with false members from the general field, and thus leads to an overestimation of the M_{orb} .

Figure 4 shows how sensitive are the $M_{orb}/\Sigma M_*$ estimates to the choice of the threshold value of Θ_1 for 15 most populous groups in the Local Volume. The variations of the $M_{orb}/\Sigma M_*$ ratio depending on Θ_1 in the range of $[-0.5 < \Theta_1 < 0.5]$ with the increments of 0.1 are shown in this figure for each of the 15 suites.

We can see from these tracks that a rapid growth of $\log(M_{orb}/\Sigma M_*)$ towards negative values of Θ_1 takes place in 5 suites only: NGC 253, NGC 4258, NGC 4594, NGC 4736, and NGC 5236. In the remaining groups (suites), the ratio of the orbital mass-to-sum of stellar masses is weakly responsive to the variation of Θ_1 . This is true in particular for the companions of the suites around the MW and M31, which are marked in the figure by solid diamonds and squares, respectively. The logarithm of the average value of $\langle M_{orb}/\Sigma M_* \rangle$ for all the groups, shown by open diamonds, varies within the range of $[1.59 - 1.67]$ when the threshold of Θ_1 changes from +0.4 to -0.4.

According to Jones et al. (2006), the mean density of stellar mass amounts to $j_* = 4.28 \times 10^8 (M_\odot/\text{Mpc}^3)$ at $H_0 = 73 \text{ km/s/Mpc}$. Assuming $M_*/L_K = 1M_\odot/L_\odot$ (Bell et al, 2003), the mean cosmic density of matter $\Omega_m = 0.28$ in the standard Λ -CDM model is expressed as $M_{DM}/M_* = 97$. This value is shown in Fig. 4 by the dashed horizontal line. As one can see, all the groups (suites), except for the NGC 3368 (Leo I group) and NGC 4594 (“Sombrero”) have the $M_{orb}/\Sigma M_*$ ratios below this value. Consequently, the amount of dark matter in the suite volumes around the massive nearby galaxies is clearly not enough to provide the cosmic density $\Omega_m = 0.28$.

The upper panel of Fig. 5 shows the distribution of 18 most populated nearby groups given in Table 2 by their total stellar masses and the projected mass estimates. The solid line corresponds to the cosmic value of $M_{DM}/M_* = 97$. As it is seen, all the nearby groups locate below the $\Omega_m = 0.28$ line, following the value which is about 3 times lower (dashed line).

A similar diagram for the orbital mass estimates of the suites is shown at the bottom panel of Figure 5. Each of the 15 populated suites (Table 1) is shown by a circle with a vertical bar, corresponding to the standard error of M_{orb} . The solid and dashed lines are fixing the values of $M_{DM}/M_* = 97$ ($\Omega_m = 0.28$) and 31 ($\Omega_m = 0.09$), respectively. The major part of the suites is concentrated near the line of $\Omega_m = 0.09$, and only two suites: NGC 3368 and NGC 4594 reside above the $\Omega_m = 0.28$ line. In addition to 15 populated suites, three small diamonds in the figure show the average values of $\langle M_{orb}/\Sigma M_* \rangle$ for the synthetic suites: L, M and S, the data on which are listed at the bottom of Table 1. Synthetic suites around the galaxies of small (S) and medium (M) mass are characterized by a high $\langle M_{orb}/\Sigma M_* \rangle$ ratio, and within the error they lie on the line of $\Omega_m = 0.28$.

Among the smallest suites, isolated pairs of dwarf galaxies can be found, where each component of the pair is the Main Disturber for the second component. The list of such 12 dwarf pairs is presented in Table 3. The low luminosity of these galaxies clearly does not favour their detection outside the Local Volume. Nevertheless, the catalog of binary galaxies in the Local Supercluster by Karachentsev & Makarov (2008) as well as the list of multiple dwarfs by (Makarov & Uklein 2012) contain about 50 more similar dwarf pairs.

The binary systems in Table 3 are ranked by their distance from us. The table columns represent the following data, adopted from the UNGC catalog: (1) names of the components; (2) the distances (Mpc); (3) tidal indices, characterizing the degree of mutual gravitational influence; (4) logarithm of stellar mass (M_\odot); (5) logarithm of the hydrogen mass (M_\odot); (6) the radial velocity difference of the components (km/s); (7) the velocity measurement error (km/s); (8) projected separation (kpc); (9) logarithm of orbital mass (M_\odot). According to these data, the average orbital mass of dwarf pairs amounts to $1.83 \times 10^{11} M_\odot$, and the average sum of stellar masses of the components is $7.7 \times 10^8 M_\odot$. The ratio of these quantities $\langle M_{orb} \rangle / \langle M_1^* + M_2^* \rangle = 237 \pm 172$ is shown in the lower panel of Fig. 5 by a square. The position of the square above the $M_{DM}/M_* = 97$ line (but with a large error bar) gives an impression that the dark-to-baryonic matter ratio tends to be higher in the low-luminosity galaxies than that in the galaxies with normal luminosity. This assertion has been repeatedly stated in the literature (Mateo 1998, Moster et al. 2010).

However, we should pay attention to two important circumstances here. The orbital mass estimates using equation (4) are statistically biased ones. In the presence of radial velocity measurement errors, the product $\langle \Delta V_{12}^2 \times R_{p12} \rangle$ in (4) should be replaced by $\langle (\Delta V_{12}^2 - \sigma_{v1}^2 - \sigma_{v2}^2) \times R_{p12} \rangle$. Accounting for the contribution of σ_{v1}, σ_{v2} errors lowers the average ratio of $\langle M_{orb} \rangle / \Sigma M_*$ to 214 ± 155 .

Comparison of stellar vs. hydrogen masses of dwarf galaxies in pairs shows that these values are comparable with each other. The mean difference $\langle \log M_{HI} - \log M_* \rangle$ from the Table 3 data is equal to -0.13 . It becomes positive, $+0.14$, if one takes into consideration that the mass of gas accounting for helium and molecular hydrogen is on the average 1.85 times larger than the mass of atomic hydrogen (Fukugita & Peebles 2004). Having introduced both the corrections, the ratio of the orbital mass-to-sum of baryonic masses of the pairs drops to $\langle M_{orb} \rangle / \Sigma(M_* + M_{gas}) = 78 \pm 56$.

Summing the stellar masses in all the considered suites of the Local Volume, we obtain $\Sigma M_* = 1.52 \times 10^{12} M_\odot$. With the average local stellar mass density of $j_* = 6.0 \times 10^8 M_\odot / \text{Mpc}^3$ (Karachentsev et al. 2013) and $M_*/L_K = 1 M_\odot / L_\odot$, the sphere of 10 Mpc radius contains the total stellar mass of $1.88 \times 10^{12} M_\odot$ (a small correction is introduced here, accounting for the zone of interstellar extinction in the Milky Way). Therefore, the studied suites contain 80% of the total stellar mass in the Local Volume. The total orbital mass for them is $8.1 \times 10^{13} M_\odot$. The $\Sigma M_{orb} / \Sigma M_* = 53$ ratio is an important dynamic characteristic of the Local Volume. The 20% of stellar mass we have unaccounted for are distributed as the field galaxies. They contribute both in the denominator and the numerator of the $\Sigma M_{orb} / \Sigma M_*$ ratio, and probably have little effect on its value. The position of the whole Local Volume in the $\log M_{orb} \propto \log M_*$ diagram is shown by a large open diamond in

the upper right corner of the bottom panel in Figure 5. The ratio of the sum of masses, equal to 53 is equivalent to the average density in the Local Volume, $\Omega_m(LV) = 0.15$.

Note, however, that more than a half of the contribution to the total value of M_{orb} in the Local Volume is introduced only by two suites around NGC 4594 and NGC 3368. Both systems are on the far edge of the Local Volume at distances of 9.3 Mpc and 10.4 Mpc, respectively. Individual distances to the majority of members of both suites are determined with an error of ~ 2 Mpc by the Tully-Fisher method, or not measured at all, being instead attributed the distance of the main galaxy of the group. Moreover, the NGC 4594 and NGC 3368 groups are located in the immediate vicinity of the “zero velocity sphere” of the Virgo cluster, where it is difficult to separate the bulk infall motions of galaxies toward the cluster from virial motions within the groups. We did not notice anything other special about their location with respect to the Local Sheet. Obviously, these groups need a more comprehensive, special analysis of their structure and kinematics with the use of new observational data.

It should be added that out of 6 members of the NGC 4594 suite, one galaxy, DDO 148, resides at the large projected distance of 1.1 Mpc from the Sombrero galaxy, having the radial velocity difference of 276 km/s. The contribution of DDO 148 to the total orbital mass estimate of the Sombrero suite is more than a half. Since the distance to DDO 148, $D = 9.0$ Mpc is determined by the Tully-Fisher method with the error of ± 2 Mpc, a more accurate estimate of its distance can dramatically change the value of M_{orb} for this suite.

If we limit the Local Volume by the 8 Mpc radius, excluding a still uncertain situation on the far boundary, the ratio of the total orbital mass of all the suites in this volume to the sum of stellar masses will be $\Sigma M_{orb}/\Sigma M_* = 30$ at $M_*/L_K = 1M_\odot/L_\odot$. On the lower panel of Fig. 5, this value, falling on the $\Omega_m = 0.09$ line is marked by a large solid diamond.

7. Masses derived from Hubble flow around the nearby groups

A high density of observational data on the radial velocities and distances of galaxies in the Local Volume gives an opportunity to determine the masses of nearby groups not only by the virial motions, but also by perturbations of the Hubble flow around them. This idea was proposed by Lynden-Bell (1981) and Sandage (1986), and is based on the measurement of the radius of the zero velocity sphere R_0 which separates a group (or a cluster) from the surrounding volume that expands.

In the standard cosmological model with the parameters $H_0 = 73$ km/s/Mpc and $\Omega_m = 0.24$ (Spergel et al. 2007) the total mass of a spherical overdensity is expressed as

$$M_T/M_\odot = 2.12 \times 10^{12} \times (R_0/\text{Mpc})^3. \quad (10)$$

An important circumstance here is that the estimate of the total mass of a group corresponds to the scale of R_0 , which is ~ 3.7 times larger than its virial radius.

The analysis of observational data on radial velocities and separations of galaxies in the vicinity of the Local Group and other nearby groups was done by different authors. A summary for six groups is presented in Table 4. The columns of the table list: (1) name of the group; (2) logarithm of the orbital mass of the group in the units of solar mass and its error; (3) radius of the zero velocity sphere (in Mpc) and its error; (4) logarithm of the total mass of the group, determined by eq. (10) and its error; (5) the difference of the total and orbital mass estimates; (6) the reference to the source of data on R_0 .

In general, the estimates of mass by two independent methods agree with each other quite well. However, a moderate systematic difference of mass estimates in favour of the orbital masses is noteworthy. For six groups the mean difference amounts to $\langle \Delta \lg(M_T/M_{orb}) \rangle = -0.20 \pm 0.05$. This paradoxical result lying in the fact that the estimates of the total mass of the groups on the scale of $R_0 \sim 3.7R_v$ are lower than the orbital (as well as the projected) mass estimates on the scale of the virial radius R_v can have a simple interpretation. Chernin et al. (2013) noted that the estimate of the total mass of a group includes two components: $M_T = M_M + M_{DE}$, where M_M is the mass of dark and baryonic matter, and M_{DE} is the mass, negative in magnitude, determined by the dark energy with the density of ρ_{DE} :

$$M_{DE} = (8\pi/3) \times \rho_{DE} \times R^3.$$

On the scale of R_v the contribution of this component in the group mass is small, not exceeding 1%. But in the sphere of R_0 radius, the role of this “mass defect” becomes significant. In the standard Λ CDM model with $\Omega_m = 0.24$ the contribution of dark energy is

$$(M_{DE}/M_\odot) = -0.85 \times 10^{12} \times (R_0/\text{Mpc})^3, \tag{11}$$

i.e. about 40% of the value determined by eq. (10). A correction to the total mass by a factor of 1.4 can almost completely eliminate the observed discrepancy between the group mass estimates at different scales.

In turn, such an agreement of mass estimates by the internal and external motions after the correction for the dark energy component can be interpreted as another empirical evidence for the existence of the dark energy itself appearing in the dynamics of nearby groups.

8. Concluding remarks

The high-density data on the distances and radial velocities of ~ 800 most nearby galaxies from the UNGC catalog provides an unique opportunity to investigate the distribution of light and dark matter in the Local Volume of ~ 10 Mpc radius in outstanding detail. The analysis of these

data shows that about a half of the population of the Local Volume is concentrated in the rooms, dominated by the gravitational influence of only 15 most massive galaxies. Ranking the galaxies by the magnitude of tidal force allows to group small galaxies in suites around their Main Disturbers. Assuming the Keplerian motions of the companions around the central galaxy with a typical orbit eccentricity of $e^2 = 1/2$, we have determined the orbital masses of the main galaxies in the Local Volume, as well as the total mass of less populated suites. Wherein, we did not use any restrictions on the radial velocity of companions relative to their main galaxy in the suites.

For the mass of dark halo around the MW and around M31, we have obtained the values of (1.35 ± 0.47) and (1.76 ± 0.33) in the units of $10^{12} M_\odot$, respectively. Analyzing the mass estimates of these galaxies, made by various authors and via different methods, Shull (2014) has concluded that the virial masses of MW and M31 amount to (1.6 ± 0.4) and $(1.8 \pm 0.5)(\times 10^{12} M_\odot)$, what is in a remarkable agreement with our estimates. The total mass of the Local Group from our data is $(3.1 \pm 0.6)(\times 10^{12} M_\odot)$. This estimate is consistent with the (MW + M31) mass estimate by Partridge et al. (2013) and Gonzalez et al. (2013) obtained based on the timing argument.

Within the Local Volume, there are 18 groups identified with the suites, for which MK11 estimated the virial (projected) masses M_p . On average, the agreement between the orbital and projected mass estimates for the suites and groups proves to be quite satisfactory. The typical ratio of both the orbital or the projected mass-to-sum of stellar masses of galaxies forming the group amounts to $M_{orb}/\Sigma M_* \simeq 30$.

Among the smallest suites in the Local Volume there are 12 isolated dwarf pairs, where each galaxy with a characteristic stellar mass of $\sim 10^8 M_\odot$ is the MD for the second component. The average ratio of the orbital mass- to-sum of stellar masses for them, $\langle M_{orb}/\Sigma M_* \rangle = 237 \pm 172$, looks a little more than that for the suites around luminous galaxies. However, taking account of a significant gas component in these small binary systems leads to the baryonic ratio of $\langle M_{orb}/\Sigma(M_* + M_{gas}) \rangle = 78 \pm 56$, close to the typical one of the galaxies with normal luminosities.

The distortion in the Hubble flow, observed around six most nearby groups allows us to determine their total masses. Independent estimates of total masses via the radius of zero velocity sphere R_0 are slightly lower than the orbital and virial values. This difference may be due to the local effect of dark energy, which affects the kinematics of the galaxy groups, especially scattered ones.

The data we have obtained on the orbital masses of suites/groups, summed over the Local Volume of the 8 Mpc radius, yield the ratio of dark-to-luminous matter of $\Sigma M_{orb}/\Sigma M_* \simeq 30$, which corresponds to the mean local density of $\Omega_m \simeq 0.09$. It seems difficult to indicate the precise error of this value, because the error is rather dominated by systematic effects than by random statistics. The present result is in line with the measurement $\Omega_m = 0.08 \pm 0.02$, derived by MK11 within a volume of the Local Supercluster ($D < 50$ Mpc) using an independent approach to find galaxy groups. Therefore, a threefold divergence between the local and global values of Ω_m , noted by many authors, remains to be an unsolved mystery of the near-field cosmology.

Acknowledgments

We thank the anonymous referee for thorough reading the manuscript and valuable comments. This work was supported by the grant of the Russian Foundation for Basic Research 13–02–90407 Ukr-f-a and the grant of the Ukraine F53.2/15. IK acknowledge the support for proposals GO 12877 and 12878 provided by NASA through grants from the Space Telescope Science Institute.

References

- Bahcall N.A., Kulier A., 2014, MNRAS, 439, 2505
- Bahcall N.A., Cen R., Dave R., et al. 2000, ApJ, 541, 1
- Bahcall J.N., Tremaine S., 1981, ApJ, 244, 805
- Barber C., Starkeburg E., Navarro J.F., et al. 2014, MNRAS, 437, 959
- Bell E.F., McIntosh D.H., Katz N., Weinberg M.D., 2003, ApJS, 149, 289
- Beloborodov A.M., Levin Y., 2004, ApJ, 613, 224
- Belokurov, V., Zucker, D. B., Evans, N. W., et al. 2006, ApJL, 647, L111
- Bond J.R., Kofman L., Pogosyan D., 1996, Nature, 380, 603
- Cautun M., van de Weygaert R., Jones B.J.T., Frenk C.S., 2014, arXiv:1401.7866
- Chernin A.D., Bisnovatyi-Kogan G.S., Teerikorpi P., et al. 2013, A&A, 553, 101
- Crook A.C., Huchra J.P., Martimbeau N. et al., 2007, ApJ, 655, 790
- Einasto J., Hutsi G., Saar E., et al. 2011, A&A, 531A, 75
- Fukugita, M., & Peebles, P. J. E. 2004, ApJ, 616, 643
- Gonzalez R.E., Kravsov A.V., Gnedin N.Y., 2013, arXiv:1312.2587
- Heisler J., Tremaine S., Bahcall J. N., 1985, ApJ, 298, 8
- Huchra J.P., Geller M.J., 1982, ApJ, 257, 423
- Ibata, R., Martin, N. F., Irwin, M., et al. 2007, ApJ, 671, 1591
- Jones D. H., Peterson B. A., Colless M., Saunders W., 2006, MNRAS, 369, 25
- Karachentsev I.D., Kaisina E.I., Makarov D.I., 2014a, AJ, 147, 13
- Karachentsev I.D., Tully R.B., Wu P.F., Shaya E.J., Dolphin A.E., 2014b, ApJ, 782, 4
- Karachentsev I.D., Makarov D., Kaisina E., 2013, AJ, 145, 101
- Karachentsev I.D., Kashibadze O.G., Makarov D.I., Tully R.B., 2009, MNRAS, 393, 1265
- Karachentsev I.D., Makarov D.I., 2008, Astrophys. Bulletin, 63, 299

- Karachentsev I.D., Tully R.B., Dolphin A.E., et al. 2007, *AJ*, 133, 504
- Karachentsev I.D., Kashibadze O.G., 2006, *Astrophysics*, 49, 3
- Karachentsev I.D., 2005, *AJ*, 129, 178
- Karachentsev I.D., Sharina M.E., Dolphin A.E., Grebel E.K., 2003a, *A&A*, 408, 111
- Karachentsev I.D., Grebel E.K., Sharina M.E., et al. 2003b, *A&A*, 404,93
- Karachentsev I.D., 1966, *Astrophysics*, 2, 159
- Knebe A., Libeskind N.I., Doumler T., et al. 2011, *MNRAS*, 417L, 56
- Libeskind N.I., Hoffman Y., Forero-Romero J., et al, 2013, *MNRAS*, 428, 2489
- Libeskind N.I., Yepes G., Knebe A., et al, 2010, *MNRAS*, 401, 1889
- Lokas E.L., Mamon G.A., 2001, *MNRAS*, 321, 155
- Lynden-Bell D., 1981, *Observatory* 101, 111
- Magtesian A., 1988, *Astrofizika*, 28, 150
- Makarov D.I., Makarova L.N., Uklein R.I., 2013, *AstBu*, 68, 125
- Makarov D.I., Uklein R.I., 2012, *Astr. Bull.*, 67, 135
- Makarov D.I., Karachentsev I.D., 2011, *MNRAS*, 412, 2498 (=MK11)
- Martin, N. F., McConnachie, A. W., Irwin, M., et al. 2009, *ApJ*, 705, 758
- Mateo M., 1998, *ARA&A*, 36, 435
- Moster B.P., Somerville R.S., Maubetsch C., et al. 2010, *ApJ*, 710, 903
- Partridge C., Lahav O., Hoffman Y., 2013, *MNRAS*, 436L, 45
- Rood H.J., Rothman V.C.A., Turnrose B.E., 1970, *ApJ*, 162, 411
- Sandage A., 1986, *ApJ* 307, 1
- Shandarin S.F., Sheth J.V., Sahni V., 2004, *MNRAS*, 353, 162
- Shull J.M., 2014, *ApJ*, 784, 142
- Spergel D.N., et al. 2007, *ApJS*, 170, 377
- Tully R.B., 1987, *ApJ*, 321, 280
- Vennik J., 1984, *Tartu Astron. Obs. Publ.*, 73, 1
- Willman, B., Dalcanton, J. J., Martinez-Delgado, D., et al. 2005, *ApJL*, 626, L85
- Wojtak R., 2013, *A & A*, 559, 89

Zavala J., Jing Y.P., Faltenbacher A., et al, 2009, ApJ, 700, 1779

Table 1: Basic properties of the nearby galaxy suites

Main galaxy	N_v	$\langle R_p \rangle$	$\langle dV \rangle$	M^*_{MD}	$\langle M_{orb} \rangle$	
(1)	(2)	(3)	(4)	(5)	(6)	
Milky Way	27	121	84	5.0	1.35	± 0.47
M31	39	198	93	5.4	1.76	± 0.33
MW + M31	66	167	89	5.2	1.56	
M81	26	219	116	8.5	4.89	± 1.41
N5128	15	343	110	8.1	6.71	± 2.09
N4594	6	577	153	20.0	28.47	± 17.80
N3368	20	408	150	6.8	17.00	± 4.30
N4258	11	316	96	8.7	3.16	± 1.01
N4736	14	515	50	4.1	2.67	± 0.90
N5236	10	294	57	7.2	1.06	± 0.28
N253	7	500	51	11.0	1.51	± 0.59
N3115	6	215	82	8.9	3.43	± 2.00
M101	6	167	76	7.1	1.47	± 0.67
IC342	8	321	66	4.0	1.81	± 0.82
N3627	7	254	69	10.2	1.45	± 0.39
N6946	6	163	60	5.8	0.66	± 0.34
All 13	142	332	96	8.5	6.27	
Synth all	89	188	69	2.6	2.74	± 0.77
Synth L	30	352	73	6.3	5.76	± 2.09
Synth M	29	156	79	1.3	2.08	± 0.68
Synth S	30	56	55	0.18	0.34	± 0.13

The columns contain: (1) name of the suite/group by its main galaxy, (2) the number of physical ($\Theta_1 \geq 0$) members of the group with measured radial velocities, (3) the average projection separation of the companions from the main galaxy (kpc), (4) the mean absolute value of the radial velocity difference of the companions relative to the main galaxy (km/s), (5) the main galaxy stellar mass in the units of $10^{10} M_\odot$, (6) the value of orbital mass of the group (suite) with the standard error in units of $10^{12} M_\odot$. The location of suites in Table 1 corresponds to their breakdown in the three panels of Fig. 1: the first lines contain the data for the MW and M31 groups, followed by the characteristics of 13 other most populated groups of the Local Volume, and the end of the table shows the average parameters of a composite (synthetic) suite.

Table 2: The nearby suites common with the MK(2011) groups

Group Suite	N_V	D_H	σ_V	R_h	$\log M_*$	$\log M_p$	$\log M_p/M_*$	T	ΔM_{12}	Θ_1	Θ_5	Θ_J
(1)	(2)	(3)	(4)	(5)	(6)	(7)	(8)	(9)	(10)	(11)	(12)	(13)
	N_V	D_{MD}	ΔV	R_{12}	$\log M_*$	$\log M_{orb}$	$\log M_{orb}/M_*$					
N253	6 8	5.1 3.9	87 64	275 500	11.24 11.07	12.87 12.18	1.63 1.11	5	3.66	-0.3	0.2	0.7
N628	6 5	11.4 7.3	46 82	171 230	10.71 10.32	12.18 12.20	1.47 1.88	5	4.96	-0.4	-0.2	-0.5
N672	5 4	7.7 7.2	41 67	74 105	9.78 9.87	11.39 11.66	1.61 1.79	5	1.78	3.8	3.8	0.2
N891	18 4	10.6 9.8	60 35	197 607	11.30 10.96	12.64 11.90	1.34 0.94	3	0.30	-0.9	-0.5	-0.1
N2903	4 5	5.7 8.9	31 45	69 197	10.42 10.82	11.62 11.68	1.20 0.86	4	5.64	1.6	1.6	-0.8
M81	30 27	2.6 3.6	138 133	102 219	10.86 11.11	12.59 12.69	1.73 1.58	3	0.81	2.5	2.6	1.5
N3115	5 7	6.0 9.7	58 113	119 215	10.53 10.96	12.29 12.54	1.76 1.57	-1	4.17	2.2	2.5	0.2
N3379	27	10.2	233	179	11.47	13.23	1.76	2	0.05	1.2	1.5	2.1
N3368	21	10.4	175	408	11.13	13.23	2.10					
N3627	16 8	10.0 10.3	154 78	192 254	11.43 11.11	13.05 12.16	1.62 1.05	4	0.19	1.1	1.3	2.0
N4258	15 12	7.6 7.8	80 127	254 316	10.97 10.97	12.45 12.50	1.48 1.53	4	2.34	1.2	1.4	1.0
N4594	11 7	11.7 9.3	61 188	597 577	11.53 11.30	12.90 13.45	1.37 2.15	1	2.98	2.7	2.8	-0.4
N4631	28 5	8.7 7.4	90 191	243 338	11.12 10.54	12.98 13.24	1.86 2.70	7	0.25	1.8	1.8	1.0
N4736	5 15	4.8 4.7	16 66	338 515	10.64 10.72	11.34 12.43	0.70 1.70	2	5.49	-0.6	-0.1	0.8
N5128	15 16	4.1 3.8	94 137	402 343	11.21 11.17	12.52 12.83	1.31 1.66	-2	0.52	0.7	1.0	1.6
N5194	9 4	7.9 8.4	84 53	182 167	11.29 11.12	12.93 11.78	1.64 0.66	4	0.12	0.0	0.4	1.3
N5236	12 11	4.4 4.9	77 61	149 294	10.78 10.87	12.29 12.02	1.51 1.15	5	3.63	-0.5	0.0	0.0
M101	6 7	5.2 7.4	61 81	150 167	10.56 10.86	12.05 12.17	1.49 1.30	6	3.97	0.3	0.5	0.2
N6744	9 4	10.3 8.3	78 90	229 401	11.12 10.94	12.59 12.70	1.47 1.75	4	1.11	2.0	2.0	1.1
Mean	13 9	7.4 7.4	83 99	218 325	10.94 10.88	12.44 12.41	1.50 1.53	3	2.33	1.0	1.2	0.7

The columns contain: (1) name of the main galaxy of the group/suite; (2) the number of galaxies in the group/suite with measured radial velocities; (3) the distance to the group (Mpc), determined by the mean radial velocity of the group members relative to the Local Group centroid at $H_0 = 73$ km/s/Mpc, and the individual distance of the principal galaxy of the suite; (4) dispersion of radial velocities in the group and the mean-square difference of the companion velocities relative to the main galaxy (km/s); (5) the mean harmonic radius of the group and the mean projection separation of the companions from the main galaxy (kpc); (6) logarithm of the total stellar mass of the group or a suite (in M_\odot); (7) logarithm of the projected mass of the group and the orbital mass of the suite (in M_\odot); (8) the ratio of the projected/orbital mass-to-total stellar mass in the logarithmic scale; (9) morphological type of the main galaxy on de Vaucouleurs scale; (10) the difference between the apparent K-magnitudes of the first and second members of the group; (11–13) the tidal indices, characterizing the density of the environment of the main galaxy of the group: here the Θ_1 index, determined by equation (6), expresses the contribution of the most significant neighbor, the Θ_5 index accounts for the effect of five important neighbors, while the Θ_J index corresponds to the logarithm of the stellar density contrast in a sphere of 1 Mpc radius around the main galaxy taken with respect to the mean cosmic density.

Table 3: Isolated binary dwarfs

Name	D	Θ_1	$\log M_*$	$\log M_{HI}$	ΔV	σ_V	R_p	$\log M_{orb}$
(1)	(2)	(3)	(4)	(5)	(6)	(7)	(8)	(9)
N3109	1.32	0.2	8.57	8.37	44	2	27	10.04
Antlia	1.32	2.3	6.47	5.92		1		
Dwing2	3.0	2.8	8.35	8.01	35	2	13	10.27
MB3	3.0	3.0	8.09	7.78		1		
KKR 59	5.9	1.7	9.16	-	11	4	36	9.70
KKR 60	5.9	2.5	8.42	-		7		
ESO121-20	6.0	-0.1	7.78	7.94	33	5	6	9.85
LV0616-57	6.0	0.6	7.07	7.36		4		
UGC2716	6.4	-0.8	8.34	7.68	29	1	112	11.04
UGC2684	6.5	-0.1	7.57	7.92		4		
KUG1202+28	6.7	0.1	7.70	-	4	33	16	8.49
LV1205+281	6.7	0.5	7.37	-		14		
DDO 64	7.1	1.6	8.04	8.24	18	2	4	9.21
KK 78	7.1	2.8	6.92	7.35		4		
DDO161	7.3	1.5	8.91	8.99	10	18	40	9.67
UGCA319	7.3	2.2	8.22	7.97		4		
MAPS1206+31	7.4	-0.4	7.81	-	4	27	44	8.92
LV1207+3133	7.4	0.2	7.12	-		4		
NGC1156	7.8	-0.3	9.31	8.82	64	1	80	11.58
LV0300+25	7.8	1.6	7.34	6.20		3		
NGC1744	10.0	0.1	9.42	9.35	90	2	169	12.20
ESO486-21	10.0	0.8	8.74	8.47		18		
KK 94	10.4	2.3	7.34	7.69	12	1	7	9.08
LeG 21	10.4	2.8	6.90	7.09		1		

The table columns represent the following data, adopted from the UNGC catalog: (1) names of the components; (2) their distances (Mpc); (3) tidal indices, characterizing the degree of mutual gravitational influence; (4) logarithm of stellar mass (M_\odot); (5) logarithm of the hydrogen mass (M_\odot); (6) radial velocity difference of the components (km/s); (7) velocity measurement error (km/s); (8) projected separation (kpc); (9) logarithm of orbital mass (M_\odot).

Table 4: Total masses of nearby groups via internal and external motions

Group	$\log(M_{orb})$	R_0	$\log(M_T)$	$\log(M_T/M_{orb})$	Reference
(1)	(2)	(3)	(4)	(5)	(6)
MW+M31	12.50±0.08	0.98 ±0.03	12.30 ±0.05	-0.20 ±0.09	Karachentsev et al. 2009
IC342	12.26±0.21	0.90 ±0.10	12.19 ±0.14	-0.07 ±0.25	Karachentsev et al. 2003a
M81	12.69±0.13	1.05 ±0.07	12.39 ±0.09	-0.30 ±0.16	Karachentsev & Kashibadze 2006
N5128+N5236	12.89±0.14	1.26 ±0.15	12.63 ±0.15	-0.23 ±0.21	Karachentsev et al. 2007
N253	12.18±0.18	0.70 ±0.10	11.86 ±0.18	-0.32 ±0.25	Karachentsev et al. 2003b
N4736	12.43±0.15	1.04 ±0.20	12.38 ±0.24	-0.05 ±0.28	Makarov et al. 2013

The columns of table list: (1) name of the group; (2) logarithm of the orbital mass of the group in the units of solar mass and its error; (3) radius of the zero velocity sphere (in Mpc) and its error; (4) logarithm of the total mass of the group, determined by eq. (10) and its error; (5) the difference of the total and orbital mass estimates; (6) the reference to the source of R_0 data.

Table 5. The tidal indices, Θ_1 , projected separation, R_p , and radial velocity differences, dV , for members of suites around 15 nearby luminous galaxies.

M81			
$D=3.63$ Mpc, $M_* = 8.51 \times 10^{10} M_\odot$, $M_{orb} = (4.89 \pm 1.42) \times 10^{12} M_\odot$			
Name	Θ_1	R_p	$ dV $
1 HolmIX	5.1	11	88
2 ClumpI	4.2	24	129
3 KDG061	4.0	31	256
4 [CKT2009]d0959+68	4.0	35	150
5 ClumpIII	3.9	39	85
6 NGC2976	2.9	88	38
7 MESSIER082	2.8	39	224
8 KDG064	2.7	103	17
9 IKN	2.5	84	105
10 HIJASS J1021+6842	2.3	147	83
11 F8D1	2.2	119	96
12 KDG063	2.0	169	104
13 DDO078	1.9	201	87
14 HolmI	1.7	157	187
15 KDG073	1.4	323	159
16 UGC05497	1.4	333	163
17 HS117	1.2	191	12
18 BK3N	1.2	12	3
19 DDO082	1.1	215	103
20 [CKT2009]d0958+66	1.0	142	117
21 IC2574	1.0	193	79
22 KDG052	0.8	511	167
23 DDO053	0.8	525	46
24 HolmII	0.7	536	207
25 UGC04483	0.6	440	200
26 KKH37	0.0	1030	110

M31			
$D = 0.77$ Mpc, $M_* = 5.37 \times 10^{10} M_\odot$, $M_{orb} = (1.76 \pm 0.33) \times 10^{12} M_\odot$			
Name	Θ_1	R_p	$ dV $
1 MESSIER032	6.6	5	93
2 And IX	4.0	36	77
3 And XVII	3.6	43	51

Table 5—Continued

4 NGC0205	3.6	8	76
5 And I	3.4	44	87
6 And III	3.2	67	53
7 And XXVII	3.0	57	232
8 And XV	2.9	92	50
9 And XXV	2.9	81	199
10 And XXVI	2.8	101	50
11 NGC0147	2.8	100	114
12 And XI	2.7	101	138
13 And XII	2.6	94	274
14 And V	2.6	109	114
15 And XXIII	2.4	126	23
16 And XX	2.4	125	153
17 And XIII	2.4	115	82
18 And XXX	2.3	114	165
19 And XXI	2.2	122	44
20 And X	2.2	76	124
21 And XIV	2.2	160	211
22 Bol520	2.0	115	35
23 And II	2.0	140	69
24 NGC0185	2.0	96	102
25 And XXIX	2.0	188	106
26 And XIX	1.9	104	186
27 And XXIV	1.9	111	156
28 MESSIER033	1.7	203	63
29 Cas dSph	1.7	223	24
30 IC0010	1.6	256	33
31 And XVI	1.5	129	114
32 LGS 3	1.5	279	45
33 Peg dSph	1.4	277	55
34 And XXVIII	1.1	407	3
35 Pegasus	0.9	463	89
36 IC1613	0.7	634	60
37 And XVIII	0.4	112	15
38 Cetus	0.3	1002	55
39 WLM	0.0	1209	13

Table 5—Continued

MW			
$D = 0.01 \text{ Mpc}, M_* = 5.00 \times 10^{10} M_\odot, M_{orb} = (1.35 \pm 0.47) \times 10^{12} M_\odot$			
Name	Θ_1	R_p	$ dV $
1 Sag dSph	5.3	5	169
2 Segue 1	4.3	17	111
3 UMa II	3.9	21	33
4 BootesII	3.8	37	116
5 Segue 2	3.8	22	43
6 Willman1	3.7	34	36
7 Comal	3.7	40	82
8 BootesIII	3.6	49	241
9 LMC	3.5	49	84
10 Umin	3.2	59	93
11 BootesI	3.2	66	106
12 Draco	2.9	80	101
13 Sculptor	2.7	90	72
14 SexDSph	2.7	85	75
15 Carina	2.6	99	13
16 UMa I	2.5	84	7
17 Hercules	2.1	107	145
18 Fornax	2.1	137	60
19 LeoIV	2.0	160	10
20 CVnII	2.0	160	96
21 LeoV	1.8	180	58
22 LeoII	1.6	201	32
23 CvnI	1.5	220	78
24 LeoI	1.4	223	175
25 LeoT	0.7	338	57
26 Phoenix	0.7	440	142
27 NGC6822	0.5	257	43

NGC5128			
$D = 3.75 \text{ Mpc}, M_* = 8.13 \times 10^{10} M_\odot, M_{orb} = (6.71 \pm 2.09) \times 10^{12} M_\odot$			
Name	Θ_1	R_p	$ dV $
1 ESO324-024	2.9	104	38

Table 5—Continued

2 ESO269-066	2.0	190	218
3 NGC5011C	2.0	148	84
4 ESO270-017	1.8	198	273
5 KK196	1.6	141	180
6 KK211	1.6	242	50
7 NGC5237	1.2	146	188
8 ESO325-011	1.1	248	1
9 NGC5206	1.0	350	24
10 KK221	1.0	376	42
11 NGC4945	0.9	482	11
12 NGC5102	0.8	422	83
13 ESO383-087	0.6	549	202
14 PGC051659	0.3	768	133
15 NGC5253	0.3	779	117

NGC4594

$D = 9.30$ Mpc, $M_* = 19.95 \times 10^{10} M_\odot$, $M_{orb} = (28.47 \pm 17.80) \times 10^{12} M_\odot$

Name	Θ_1	R_p	$ dV $
1 SUCD1	6.5	8	215
2 KKSG30	1.2	458	23
3 LV J1235-1104	0.8	194	109
4 MCG-02-33-075	0.4	757	279
5 DDO148	0.2	1097	276
6 NGC4597	0.0	949	18

NGC3368

$D = 10.42$ Mpc, $M_* = 6.76 \times 10^{10} M_\odot$, $M_{orb} = (17.00 \pm 4.30) \times 10^{12} M_\odot$

Name	Θ_1	R_p	$ dV $
1 LeG13	3.1	82	22
2 LeG17	2.9	92	140
3 FS04	1.8	231	119
4 UGC05812	1.5	285	117
5 AGC202456	1.5	285	71
6 NGC3412	1.3	343	38
7 LeG05	1.3	346	111
8 AGC205268	1.1	390	261

Table 5—Continued

9 NGC3351	1.1	126	117
10 AGC205445	1.1	398	250
11 LSBC D640-12	1.0	419	41
12 LSBC D640-13	1.0	423	100
13 AGC200499	0.9	466	273
14 LeG06	0.8	486	123
15 NGC3299	0.8	488	287
16 UGC06014	0.8	491	232
17 AGC202248	0.7	531	280
18 AGC205156	0.3	716	22
19 AGC205165	0.2	771	154
20 LeG03	0.2	782	247

NGC4258

$D = 7.83$ Mpc, $M_* = 8.71 \times 10^{10} M_\odot$, $M_{orb} = ((3.16 \pm 1.01) \times 10^{12} M_\odot)$

Name	Θ_1	R_p	$ dV $
1 NGC4242	1.8	233	62
2 NGC4288	1.7	144	82
3 NGC4248	1.1	30	38
4 LV J1203+4739	0.9	372	41
5 KDG101	0.7	30	316
6 NGC4144	0.6	239	189
7 KK133	0.5	536	95
8 UGC07639	0.4	255	56
9 DDO120	0.3	211	10
10 MAPS1249+44	0.2	834	66
11 UGC07827	0.1	597	103

NGC4736

$D = 4.66$ Mpc, $M_* = 4.07 \times 10^{10} M_\odot$, $M_{orb} = (2.67 \pm 0.90) \times 10^{12} M_\odot$

Name	Θ_1	R_p	$ dV $
1 IC3687	1.4	252	25
2 IC4182	0.9	370	5
3 KK160	0.8	232	6
4 UGC08215	0.5	530	48
5 DDO126	0.4	497	122

Table 5—Continued

6 NGC4449	0.3	418	103
7 NGC4244	0.3	592	93
8 DDO168	0.3	525	82
9 CGCG 189-050	0.2	486	16
10 DDO169	0.2	634	4
11 DDO167	0.1	539	122
12 NGC4395	0.1	743	44
13 DDO169NW	0.0	635	24
14 MCG +06-27-017	0.0	759	11

NGC5236

$D = 4.92$ Mpc, $M_* = 7.24 \times 10^{10} M_\odot$, $M_{orb} = ((1.06 \pm 0.28) \times 10^{12} M_\odot)$

Name	Θ_1	R_p	$ dV $
1 IC4247	2.0	195	107
2 UGCA365	1.3	55	60
3 ESO444-084	1.3	157	73
4 KK200	1.2	249	36
5 NGC5264	1.1	86	38
6 KK195	0.9	326	38
7 IC4316	0.7	104	62
8 HIDEEP J1337-33	0.5	301	64
9 ESO384-016	0.4	596	43
10 HIPASS J1337-39	0.1	870	49

NGC0253

$D = 3.94$ Mpc, $M_* = 10.96 \times 10^{10} M_\odot$, $M_{orb} = (1.51 \pm 0.59) \times 10^{12} M_\odot$

Name	Θ_1	R_p	$ dV $
1 NGC0247	1.2	312	60
2 ESO540-032	0.7	374	9
3 DDO006	0.6	297	68
4 KDG002	0.5	500	14
5 NGC7793	0.2	916	26
6 DDO226	0.1	221	133
7 ESO349-031	0.0	880	46

NGC3115

Table 5—Continued

$D = 9.68 \text{ Mpc}, M_* = 8.91 \times 10^{10} M_\odot, M_{orb} = (3.43 \pm 2.00) \times 10^{12} M_\odot$			
Name	Θ_1	R_p	$ dV $
1 KDG065	4.9	15	40
2 KKSG18	3.9	48	17
3 KKSG17	2.3	175	236
4 MCG -01-26-009	1.8	254	71
5 UGCA193	1.5	309	12
6 KKSG15	0.9	488	115

M101

$D = 7.38 \text{ Mpc}, M_* = 7.08 \times 10^{10} M_\odot, M_{orb} = (1.47 \pm 0.67) \times 10^{12} M_\odot$			
Name	Θ_1	R_p	$ dV $
1 GBT 1355+5439	2.2	161	33
2 NGC5474	2.0	95	46
3 HolmIV	1.8	170	106
4 NGC5477	1.4	46	73
5 KKH87	0.9	414	95
6 UGC08882	0.0	117	104

IC342

$D = 3.28 \text{ Mpc}, M_* = 3.98 \times 10^{10} M_\odot, M_{orb} = (1.81 \pm 0.82) \times 10^{12} M_\odot$			
Name	Θ_1	R_p	$ dV $
1 KK35	2.4	16	95
2 UGCA086	1.1	90	36
3 NGC1560	1.0	313	74
4 CamB	0.9	366	23
5 NGC1569	0.9	313	138
6 Cas1	0.5	530	40
7 UGCA105	0.3	612	37
8 CamA	0.0	327	88

NGC3627

$D = 10.28 \text{ Mpc}, M_* = 10.23 \times 10^{10} M_\odot, M_{orb} = (1.45 \pm 0.39) \times 10^{12} M_\odot$			
Name	Θ_1	R_p	$ dV $
1 AGC213436	3.1	94	88
2 IC2684	2.6	143	128

Table 5—Continued

3 IC2791	2.5	149	49
4 IC2787	2.3	176	3
5 AGC215354	1.7	237	80
6 NGC3593	0.8	249	87
7 CGCG 066-109	0.4	728	50

NGC6946

$D = 5.89 \text{ Mpc}, M_* = 5.75 \times 10^{10} M_\odot, M_{orb} = ((0.66 \pm 0.34) \times 10^{12} M_\odot)$			
Name	Θ_1	R_p	$ dV $
1 KK251	3.5	59	78
2 UGC11583	3.3	65	74
3 KK252	3.1	80	86
4 KKR55	2.4	136	18
5 KKR56	1.7	238	91
6 Cepheus1	0.9	401	13

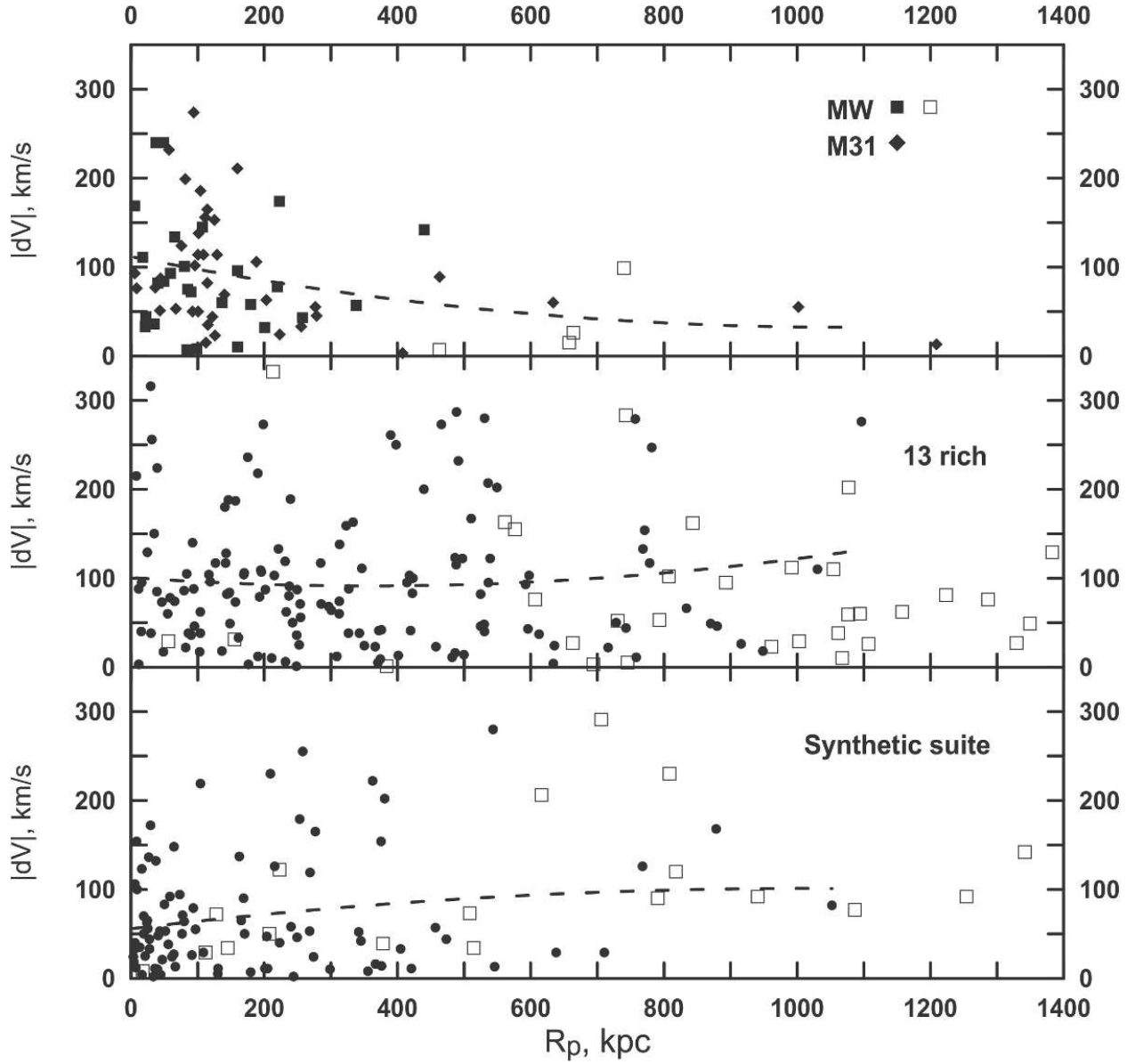


Fig. 1.— Line-of-sight velocity of the suite members relative to the main galaxy as a function of their projected linear separation. The upper panel corresponds to 70 companions of the MW (squares) and M31 (diamonds). The middle panel indicates data on 174 galaxies in 13 the most populated nearby suites. The bottom panel presents a synthetic suite formed of 107 companions around other smaller Main Disturbers. Marginal members of the suites with $\Theta_1 = [-0.5 - 0.0]$ are depicted by open squares. The dashed lines trace quadratic regressions.

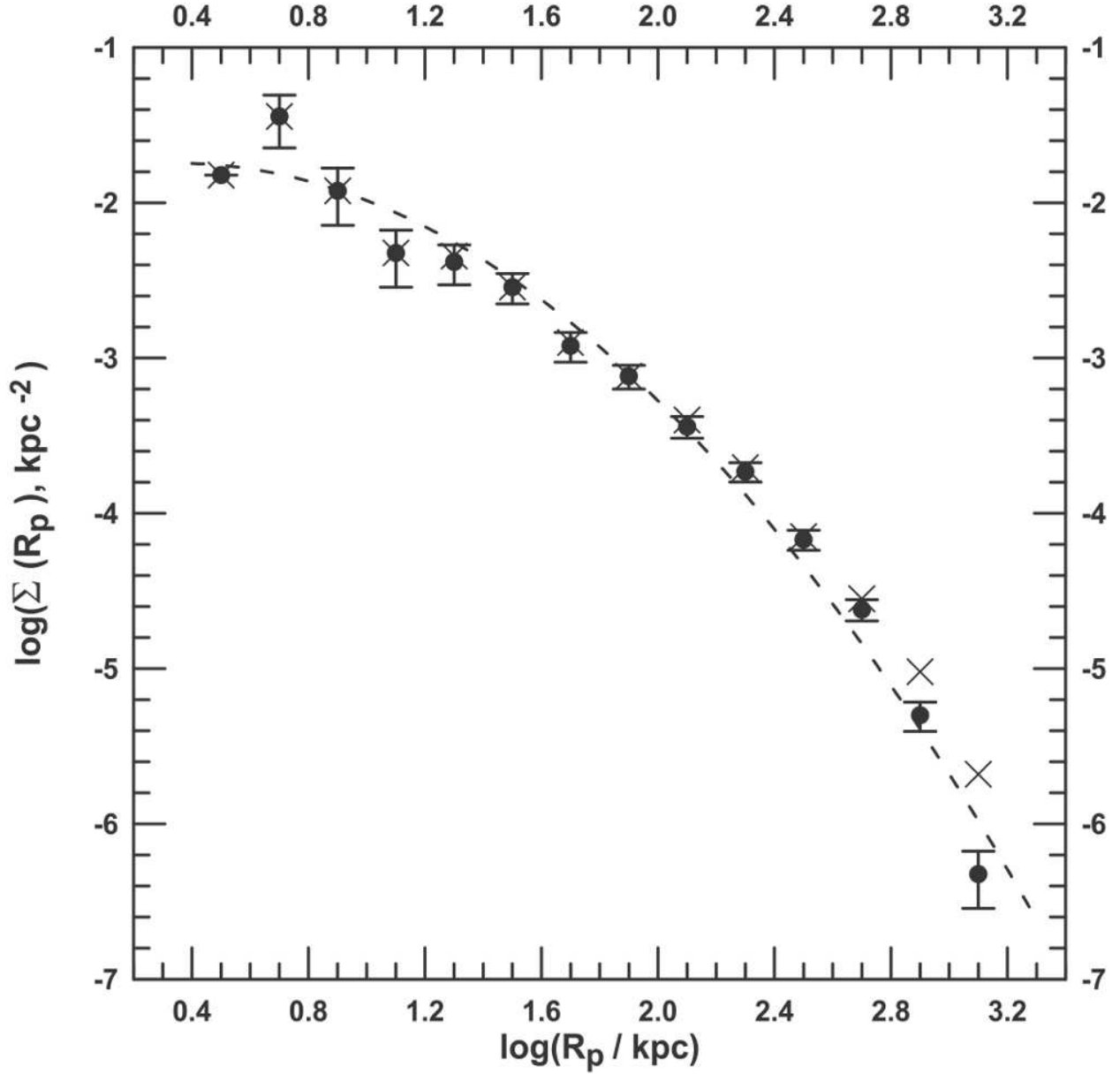


Fig. 2.— The radial profile of the surface number density of companions in the synthetic suite of the Local Volume. The solid circles represent the physical suite members with $\Theta_1 > 0$, and the crosses also account for the marginal members with $\Theta_1 = [-0.5 - 0.0]$. The dashed line fits the quadratic regression for the physical companions.

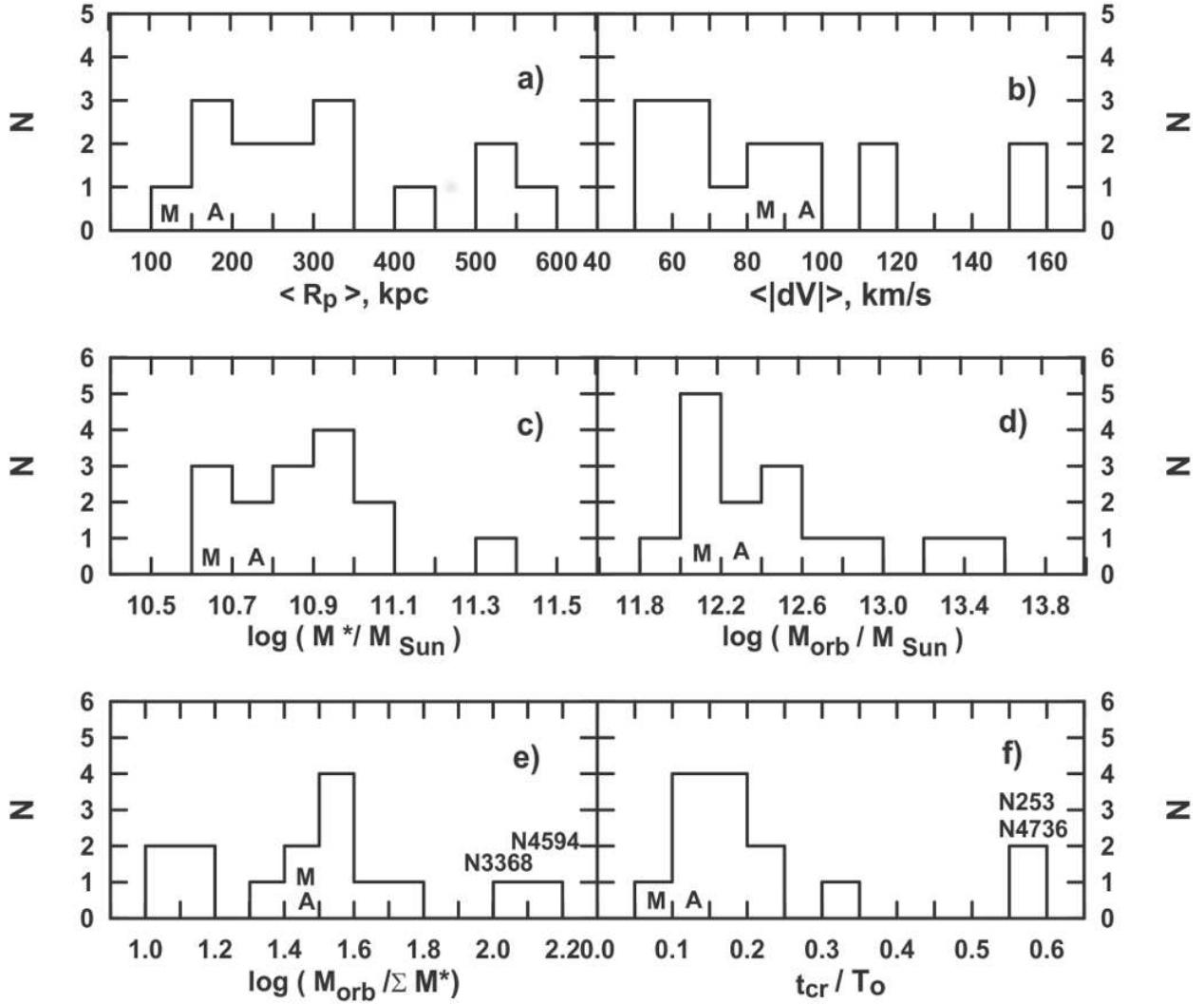


Fig. 3.— The distributions of the 15 richest nearby suites according to: a) the mean projected separation of physical companions, b) radial velocity dispersion, c) logarithm of stellar mass of the main galaxy, d) logarithm of the mean orbital mass estimate, e) the mean orbital-to-stellar mass ratio, f) the mean crossing time for the components in units of the global cosmic time T_0 . The Milky Way suite and the Andromeda (M31) suite are depicted by "M" and "A", respectively.

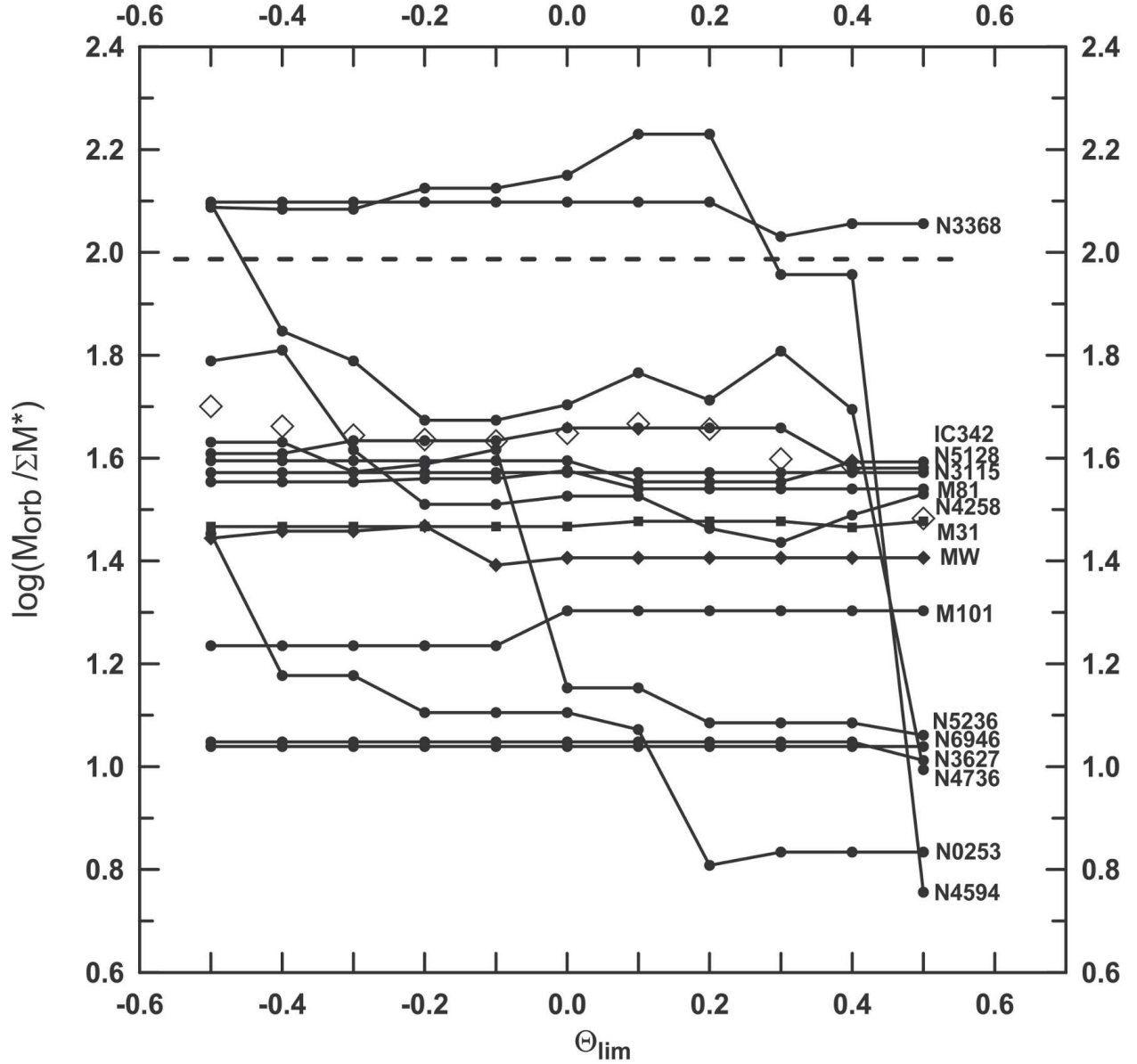


Fig. 4.— The orbital mass-to-sum of stellar mass ratio for 15 richest suites as a function of cutoff on Θ_1 . The suites of the MW and M31 are marked by solid diamonds and squares, respectively. Large open diamonds show the weighted average orbital mass-to-stellar mass ratio for the sample of 15 suites. The dashed horizontal line indicates the $M_{DM}/M_* = 97$ ratio corresponding to $\Omega_m = 0.28$.

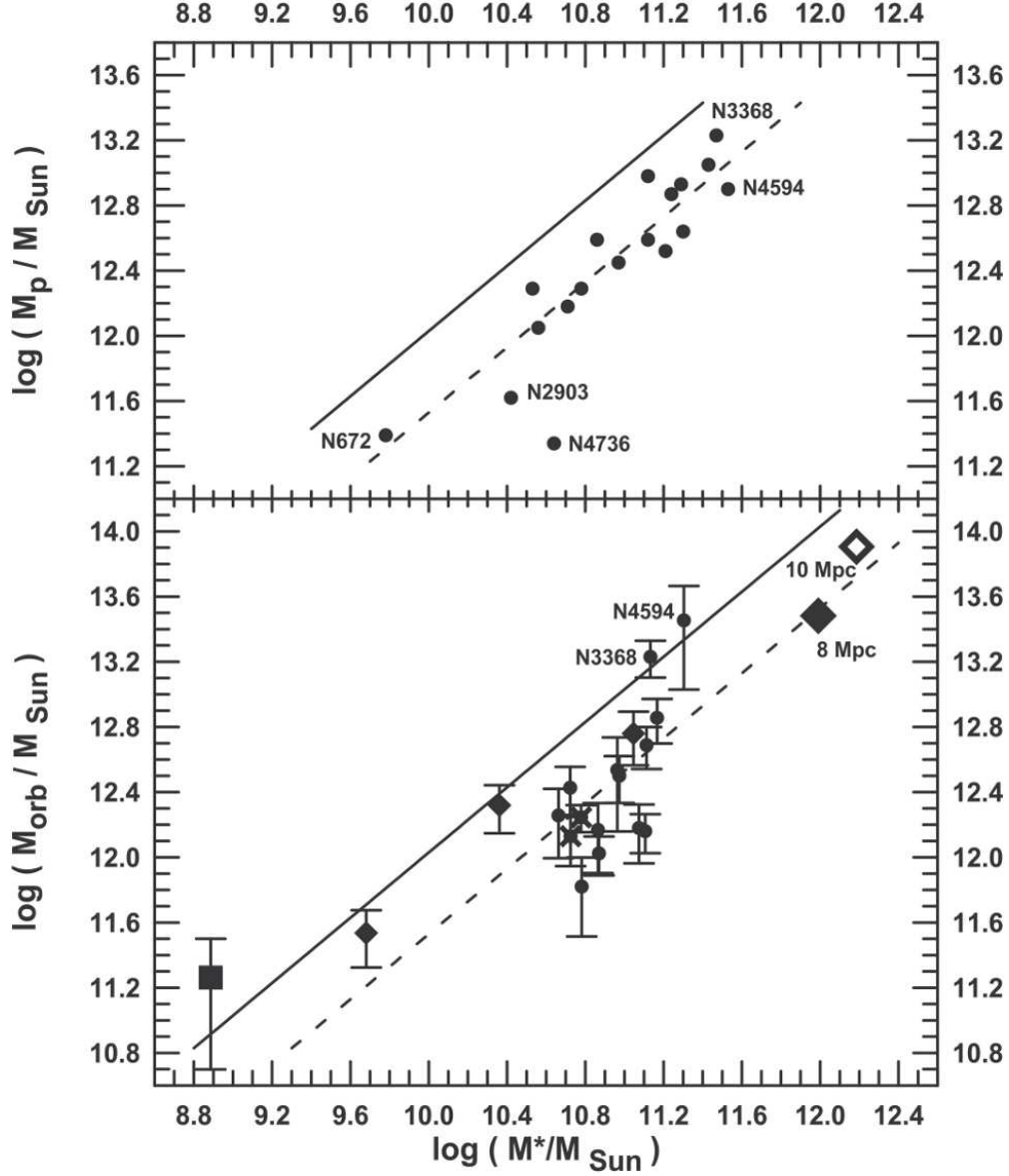


Fig. 5.— Upper panel: the projected mass of nearby groups as a function of sum of their stellar mass. Some individual groups are marked by the name of their principal member. The diagonal solid and dashed lines indicate the ratios: $M_{DM}/M_* = 97$ and 31 , respectively. Bottom panel: the orbital mass of nearby suites vs. sum of their stellar mass. Solid circles with error bars correspond to individual rich suites. The suites around the MW and M31 are marked by crosses. Small solid diamonds with error bars indicate the weighted mean ratios for the synthetic suites divided onto three sets: L (large), M (medium) and S (small) according to their Main Disturber mass. The filled square indicates the weighted average ratio for 12 isolated pairs of dwarfs. The open and filled large diamonds show the total orbital and stellar mass for the Local Volume of the radius of the 10 Mpc and 8 Mpc radius, respectively. The diagonal lines mean the same as those in the upper panel.